THE JOURNAL OF PHYSICAL CHEMISTRY C

Article

pubs.acs.org/JPCC

Do Surface Wetting Properties Affect Calcium Carbonate Heterogeneous Nucleation and Adhesion?

Nicolas R. Chevalier*

Laboratoire Matière et Systèmes Complexes UMR 7057, Université Paris Diderot, 10 rue Alice Domon et Léonie Duquet, 75013 Paris, France

Supporting Information

ABSTRACT: We study the effect of wetting properties on the propensity of a surface to heterogeneously nucleate or adsorb calcium carbonate from a saturated aqueous solution. Glass, silanized glass, and polyethylene surfaces are considered. UV-ozone is used to tune the wetting behavior from hydrophobic to hydrophilic by forming oxidized carbon groups (alcohol, aldehyde, carboxylic). For all substrates that do not promote any specific orientation of $CaCO_3$ crystals, increasing hydrophilicity inhibits $CaCO_3$ nucleation. Complete ⟨104⟩ and ⟨001⟩ crystal orientations relative to the substrate plane are obtained for silanized glass exposed to prolonged UV-ozone treatment; nucleation densities are then also considerably higher. Our results highlight the role of interfacial surface energies and orientation in heterogeneous crystal nucleation and adsorption phenomena and contribute to the rational design of antiscaling surface treatments.

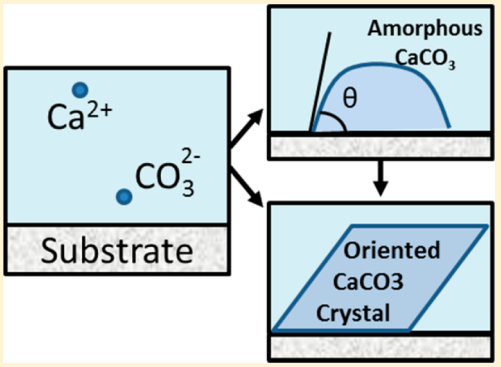

INTRODUCTION

Calcium carbonate is one of the major components of scale formation in hardwater pipes (Figure 1a), a considerable industrial issue. Scaling leads to decreased thermal conductivity in heat exchangers and increased hydraulic load losses. Their overcompensation can be the source of significant safety hazards, which has for example led Philips to withdraw 2 million coffee machines from the market in 2009 as the problem could have caused "the machine's internal boiler to burst".[1] $CaCO_3$ scales are usually dealt with after deposition, by cleaning with acids or Ca^{2+} chelants, but very often necessitate replacement of the clogged parts, which can obviously lead to significant costs, especially when pipes are poorly accessible. Scale deposition can also be prevented by various strategies,[2] e.g., Ca^{2+} sequestration (by EDTA for example, obviously not applicable to drinking water), magnetic fields[3] (their effect remains controversial), or by concentrating scale formation in a particular area (oyster shells have traditionally been placed in toilet bowls for that purpose). Although neglected so far, simple, cost-efficient surface modification processes, such as electron beam (commonly used for sterilization), UV irradiation, or thin film deposition, could potentially also be applied to reduce or postpone the onset of scale formation. This surface engineering approach requires understanding how scale deposition depends on fundamental surface properties such as surface roughness[4] and surface charge and chemistry.[5,6] In this paper, we address the fundamental question of the relation between the hydrophobic character of a surface and its propensity to nucleate and adsorb $CaCO_3$ crystals.[7,8] All of the above-mentioned surface properties can contribute to its hydrophobicity; we restrict ourselves here to the effects of surface chemistry.

In nucleation and growth phenomena, for example when considering the formation of dew, the surface free energy between the nucleated phase and the substrate plays an important role: all other parameters being equal, dew will first nucleate on the most hydrophilic parts of a surface. $CaCO_3$ crystals grow on substrates either by heterogeneous nucleation or by bulk nucleation followed by adsorption to the substrate (Figure 1b).[10] In either case, the initial substrate−solution (sub/sol) and $CaCO_3$−solution interface ($CaCO_3$/sol) is replaced by a $CaCO_3$−substrate interface ($CaCO_3$/sub), and the net surface free energy of a crystal nuclei on the surface can be written as

$$\gamma_{net} = \gamma_{CaCO_3/sol} + h(\gamma_{CaCO_3/sub} - \gamma_{sub/sol}) \quad (1)$$

where h is a shape factor and γ_{ij} are the interfacial free energies. A "$CaCO_3$-repellent" surface (high γ_{net}) would be one that is both hydrophilic (low $\gamma_{sub/sol}$) but does not form strong bonds with $CaCO_3$ crystals (high $\gamma_{CaCO_3/sub}$). Since the nucleated phase is a mineral, the interfacial free energies $\gamma_{CaCO_3/sub}$ and $\gamma_{CaCO_3/sol}$ must be specified for the different possible crystal faces.[11] Considerable attention has been devoted to low $\gamma_{CaCO_3/sub}$ substrates that strongly promote crystalline orientation using charged, ion-attracting hydrophilic surfaces, with a well-defined and homogeneous surface chemistry such as that

Received: April 18, 2014
Revised: July 15, 2014

   dx.doi.org/10.1021/jp503807v | J. Phys. Chem. C XXXX, XXX, XXX−XXX

obtained by self-assembled monolayers[12] or Langmuir–Blodgett films.[13] These investigators sought to understand how protein chemical moieties can orient crystals in biominerals (e.g., oyster shell) and what the prerequisites are for crystal orientation during solution precipitation.

Here, we set out determining in a more general way how wettability characteristics influence the propensity to nucleate $CaCO_3$, by varying the substrate surface chemistry. We consider two hydrophobic materials: thin-film silanized glass (GOTS) and bulk low-density polyethylene (PE) and hydrophilic glass slides as reference control samples. The wettability of the substrates was varied from hydrophobic to completely wettable by exposing them for different amounts of time to UV/O_3 and subsequently characterized by X-ray photoelectron spectroscopy (XPS) and contact angle measurements. After mineralization in supersaturated $CaCO_3$ solutions, the crystal number per surface area, surface coverage, crystal orientations, and polymorphs from different substrates were compared. We find that glass and silanized glass after prolonged exposure to UV/O_3 promote complete ⟨001⟩ and ⟨104⟩ orientation, respectively. They also yielded significantly higher crystal densities than PE, which did not promote any orientation of the crystals regardless of the exposure time to UV/O_3. $CaCO_3$ orientation induction on OTS and glass is discussed in the light of stereochemical or epitaxial effects investigated previously in the literature. Interestingly, for all hydrophobic substrates that did not promote crystal orientation (PE and GOTS at short exposure times), increasing the wettability causes a decrease in the amount of $CaCO_3$ deposited at the surface. These results show that wettability is an important parameter to design scale-repellent surface treatments and give fundamental insight into the mechanisms that direct surface promoted growth of crystals from solution.

EXPERIMENTAL SECTION

Silanation. Glass slides (18 × 18 mm, Prolabo, rms roughness 0.2–0.3 nm measured by tapping AFM) are thoroughly washed with soap, rinsed, sonicated for 10 min in ultrapure DI water (18.2 MΩ·cm, pH 5.8), isopropanol (Merck, 99%), and $CHCl_3$ (SDS, 99.9%), and dried in an oven (80 °C). We further eliminate residual organic contamination by exposing the glass slides to UV/O_3 for 20 min on each face. At this point, a drop of water completely spreads on the substrate surface. The substrates were then moved to a glovebox under a N_2 atmosphere and immersed in a 1 mM solution of OTS ($C_{18}H_{37}Cl_3Si$) in heptane (SDS, 99%) for 24 h. The excess OTS was thereafter removed by thoroughly washing with heptane; the slides were then taken out of the glovebox and dried. They were finally sonicated in the reverse order in $CHCl_3$, isopropanol, and water and kept in air in a sealed container for further use. The resulting average water contact angles were 97 ± 3°. Substrates were stable and could be kept for several weeks thereafter in sealed, opaque containers.

Substrate Preparation before UV/O_3 Exposure. We used glass and silanized glass (GOTS) as described above and 20 × 20 mm polyethylene squares cut from Petri dishes. All samples were first thoroughly washed with soap, rinsed, and sonicated for 10 min in isopropanol (Merck, 99%) and ultrapure DI water (18.2 MΩ·cm, pH 5.8).

UV/O_3 Exposure and Contact Angle Determination. Samples were exposed to λ = 180 and 254 nm UV light (Novascan, PSD Pro Series) for different amounts of time (0–60 min) under normal atmospheric conditions (21% O_2). The substrates were placed far (∼10 cm) from the lamp so the UV illumination would be as homogeneous as possible. Reference glass slides were always exposed for at least 20 min, resulting in a completely wettable, hydrophilic surface. To get a gradient of exposure times (for GOTS, PE), a mask made from aluminum foil was moved at regular time intervals. Substrates under the mask were not affected by ozone. Preliminary contact angle measurements were realized on separate batches at the same lamp–substrate distance. Contact angles were averaged from the values obtained for three different 5 μL drops and extracted using the LB-ADSA ImageJ plugin.[14]

XPS. X-ray photoelectron spectroscopy (XPS) analyses were performed on a separate batch of GOTS samples using a Kratos Axis-UltraDLD spectrometer, using the monochromatized Al KR line at 1486.6 eV with a power source of 150 W. Fixed analyzer pass energy of 20 eV was used for all core level scans. The photoelectron takeoff angle was 90° with respect to the sample plane, which provides an integrated sampling depth of ∼15 nm. Photoelectrons are thus collected from the entire silanized layer (thickness ∼ 2 nm). The analyzed surface was 700 μm × 300 μm. Binding energies were calibrated against the Au $4f_{7/2}$ binding energy of a gold surface at 83.90 eV.

Mineralization. Particular care was taken to devise a protocol that allowed all substrates to be subject to the same mineralization conditions, so that differences of nucleation densities could be unambiguously traced back to the surface modifications. As all samples (∼100) could not be placed in the same mineralization tank (space limitations), we performed assays separately for each material type (GOTS, PE). To make sure the mineralization results could be compared between material type, we used reference hydrophilic glass slides prepared as described above. All slides were placed immediately after UV/O_3 exposure in separate small glass beakers containing 10 mL of 10 mM $CaCl_2$ solution. The slides in the beakers are tilted at a ∼45° angle; the face of the sample exposed to UV/O_3 was oriented so it pointed downward. The beakers were then placed at random in a closed desiccator (volume ∼ 5 L), containing 1 g of ammonium carbonate ($(NH_4)_2CO_3$) for 2 h. Ammonium carbonate decomposes to form a saturated homogeneous NH_4 and CO_2 gas atmosphere above the beakers that dissolves and triggers the reactions

$$CO_2 + Ca^{2+} + H_2O \rightarrow CaCO_3 + 2H^+$$

$$2NH_3 + 2H^+ \rightarrow 2NH_4^+$$

The pH of the solution had increased from 5.6 to 8.9 after 2 h because of the buffering by NH_3^+ and CO_3^{2-}. In all assays, bulk precipitation was evidenced by the sudden appearance of a uniform white cloud in the beakers after ∼1 h and by the fact that the up pointing face of the samples had much higher crystal densities than the down-pointing one, as most $CaCO_3$ particles had sedimented after 2 h. The slides were taken out, vigorously washed in a DI water jet from a wash bottle, dried, and stored for further analysis. In most cases, $CaCO_3$ nucleation on the bottom side was homogeneous on the scale of the sample's size. Sometimes crystallization occurred before CO_2 concentrations were homogeneous across the beakers, resulting in a crystal density gradient from the bottom to the top of the sample; in this case, the whole batch was dismissed. Supersaturations reached for this vapor diffusion protocol were estimated by mineralizing clean glass reference slides using $CaCl_2$ + Na_2CO_3 mixtures. Crystal densities similar

dx.doi.org/10.1021/jp503807v | J. Phys. Chem. C XXXX, XXX, XXX–XXX

to those found using the vapor diffusion method were found for supersaturations $\sigma = \ln(a_{Ca^{2+}}a_{CO_3^{2-}}/K_{sp})$ in the range 6.2−7.6 ($a_{Ca^{2+}}$ and $a_{CO_3^{2-}}$ are the activities of calcium and carbonate ions, and K_{sp} is the solubility threshold of calcite). The mixing protocol was not further used as crystal distributions across samples were much more uniform when using the diffusion method.

Analysis. The samples were analyzed by optical microscopy. Nine distinct 1.4 mm^2 regions from the down-pointing face were photographed at random (but not near the edge) on each sample. The pictures were subsequently analyzed for particle size, number, and area coverage using ImageJ's "Analyze Particles" plugin. Results were verified and corrected when necessary (e.g., touching particles). The vaterite crystals have a distinct rounded, blossom-like morphology; we counted their number by the eye. The average over the nine regions for each sample is computed; the total length of the error bars in all plots is twice the mean standard error. Crystal orientations were determined from the three angles at the apex of the rhombohedra and were for selected samples further confirmed by X-ray diffraction (Siemens D5000) in $\theta-2\theta$ mode. In this mode, only diffracting planes parallel to the substrate surface produce significant X-ray diffraction signal, indicating the dominant orientation (Figure S4).

RESULTS

Effect of UV/O_3 Treatment. The effect of UV/O_3 treatment time t on the substrate's water contact angle is shown in Figure 2.

The contact angle decay upon increasing UV/O_3 exposure time gives us a characteristic time over which surface modifications occurred. To characterize what chemical groups are created upon UV/O_3 exposure, we performed XPS analysis of the GOTS samples. UV/O_3 treatment resulted in a steep decrease in the intensity of the peak at 285 eV (Figure 3a). This peak corresponds to C−C and C−H carbons, indicating that the alkane chains are being broken down. In parallel, three other peaks were seen to grow at 286.7, 288.3, and 289.5 eV (Figure 3a); they were ascribed[15] to alcohol (C−OH), aldehyde (C═O), and carboxylic (COOH) groups, respectively. The resulting XPS spectra were fitted with four Gaussians, and the integrated intensity of each peak as a function of exposure time was computed (Figure 3b,c). Functional groups R at the surface are seen to be produced in the order: alcohol, aldehyde, carboxylic. We further used the non-UV-treated GOTS sample to calibrate the emitted intensity per carbon atom, since we know that this sample corresponds to an 18-carbon-long monolayer of density 5.2 nm^{-2}. This enables us to compute functional group densities as a function of exposure time, as shown in Figure 3d.[16] For exposure times of 10 min and more, the XPS spectrum of GOTS was identical to that of clean hydrophilic glass, indicating that the OTS layer had vanished. This is confirmed by the complete wettability of the surface at this stage ($\theta = 0°$). For PE samples, we refer to Poullson and Mitchell,[17,18] who showed using XPS that UV/O_3 induced wettability proceeds essentially via the same functional group formation (alcohol, aldehyde, carboxylic) as those we found for GOTS. They moreover found by AFM that UV ozone has a negligible effect on surface roughness. Unlike GOTS which eventually vanishes under UV/O_3 exposure, the contact angle for bulk PE saturates at a minimum value of ~20° at high exposure times (Figure 2).

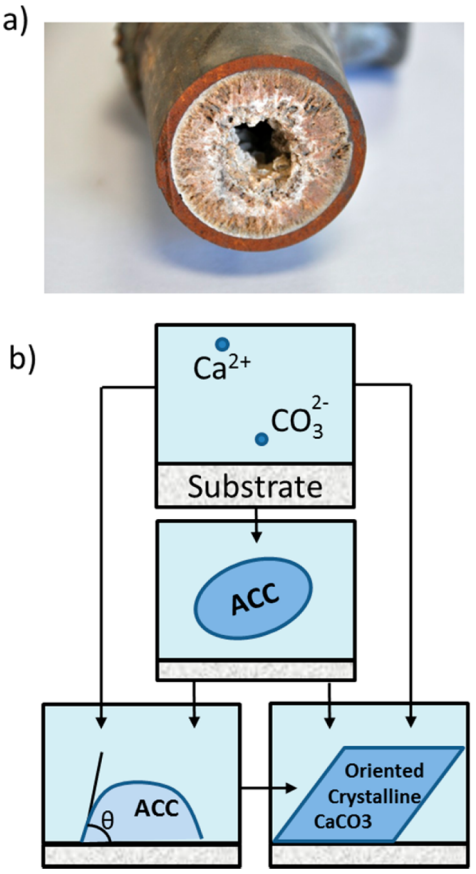

Figure 1. (a) A pipe clogged by $CaCO_3$ deposit (image courtesy of Eurodynamics Water Technologies). (b) Schematic mechanism of the formation of scales. In many instances, ions first condense as amorphous calcium carbonate (ACC) and later on transform to crystalline $CaCO_3$. The surface can promote a particular crystal orientation. Ions can crystallize out of solution either directly on the surface or in the bulk of the solution and then adhere to its surface.[9,10]

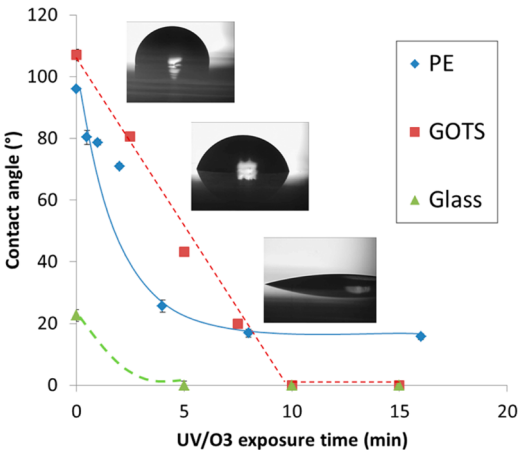

Figure 2. Water contact angle of the substrates used in this work decreases with increasing exposure to UV/O_3. Photograph insets show the contact angles on PE at 0, 2, and 8 min exposure time. Lines are guides to the eye.

Mineralization Assays. *Adhesion or Surface Nucleation ?* In all assays, crystals were present on the bottom surface of the samples only when bulk nucleation concurrently occurred. Bulk nucleation was evidenced by the large amount of sedimented particles on the top surface of the samples. Reducing $CaCl_2$

dx.doi.org/10.1021/jp503807v | J. Phys. Chem. C XXXX, XXX, XXX−XXX

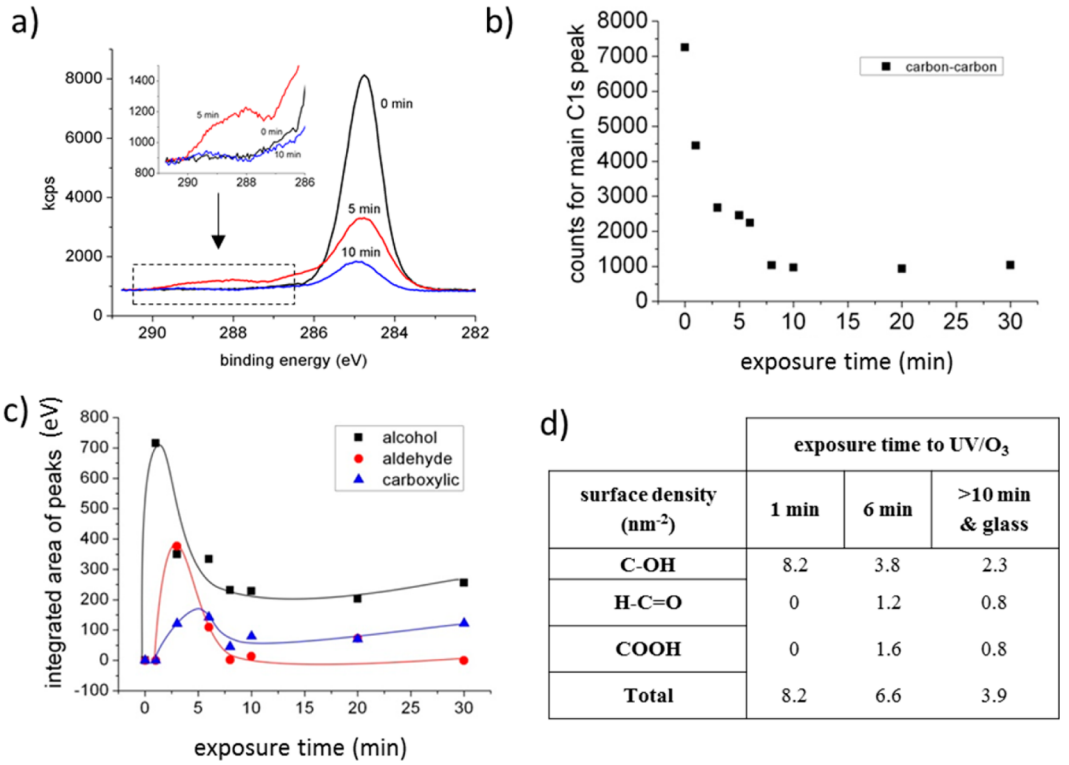

surface density (nm^{-2})	exposure time to UV/O_3		
	1 min	6 min	>10 min & glass
C-OH	8.2	3.8	2.3
H-C=O	0	1.2	0.8
COOH	0	1.6	0.8
Total	8.2	6.6	3.9

Figure 3. (a) Evolution of the XPS spectrum of GOTS with increasing exposure time. The C−C/C−H peak at 285 eV fades while other peaks corresponding to oxidized carbons appear in the region 286−290 eV; the inset shows a blow-up of this region. (b) Integrated area of the C−C/C−H peak at 285 eV as a function of exposure time, for $t \geq 10$ min; it remains constant at a value equal to that of hydrophilic glass. The remaining carbon is probably contamination, e.g., by reactions with CO_2. (c) Alcohol, aldehyde, and carboxylic group relative amounts as obtained from the fitting procedure described in the text. (d) Moiety surface densities (molecules/nm^2) for different exposure times.

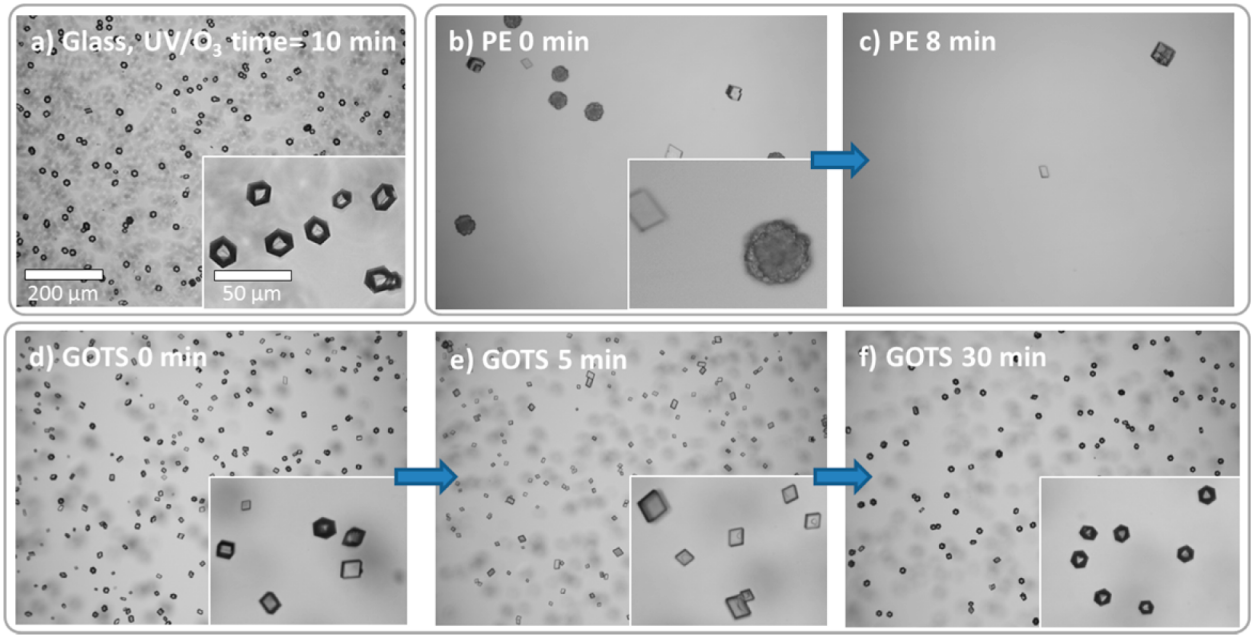

Figure 4. Optical microscopy images of the crystals obtained on each surface type for different UV/O_3 exposure times. (a) Mineralization on clean hydrophilic glass slides is almost completely ⟨001⟩ oriented, with high nucleation densities. Scale bars are the same as in (a) for all pictures and insets in this figure. (b) Untreated PE nucleates significant amounts of vaterite; calcite shows no preferred orientation. (c) UV/O_3 treated PE exhibits reduced crystal densities. (d) Crystals on an untreated silane layer are mostly calcite with no obvious preferred orientation. (e) On silane with $\theta \sim 45°$ (5 min exposure to UV/O_3) completely ⟨104⟩ oriented calcite is nucleated. (f) When the silane layer is almost completely removed by UV/O_3 ($\theta \sim 0°$, 30 min exposure time), the ⟨001⟩ orientation of calcite on clean glass is recovered as in (a).

concentrations below the homogeneous nucleation threshold resulted in no crystals on the substrates; no regime could be evidenced where only heterogeneous nucleation occurred. $CaCO_3$ crystals therefore either nucleate directly on the

dx.doi.org/10.1021/jp503807v | J. Phys. Chem. C XXXX, XXX, XXX−XXX

substrate surface or by bulk (solution) nucleation followed by adsorption to the substrate: as these two situations are difficult to separate experimentally, we will further refer to them without distinction as "surface promoted" nucleation or adsorption. Using the vapor diffusion method and concentrations similar to ours, Rieke and colleagues[10] provide compelling evidence for the fact that crystal polymorph/orientation can still be influenced even when crystal growth occurs by adsorption from the bulk. As will be shown further, the substrates we used exerted a considerable influence on densities, crystal orientations, and polymorphs. No evidence for a particle adsorption scenario has been found at lower supersaturations[19] ($\sigma < 4.9$).

Crystal number density σ (nm^{-2}) was considered a good measure of the propensity of the substrate to promote crystal growth; crystal surface coverage, s, measured as the area ratio of surface occupied by $CaCO_3$ divided by the total surface area, is a result of both nucleation/adsorption and subsequent growth. As crystal size l across any given sample was fairly homogeneous, the surface coverage is roughly proportional to the product of crystal density by average crystal size, i.e., $s \propto \sigma l$.

Glass. Clean hydrophilic glass favored ⟨001⟩ oriented calcite crystals (Figure 4a) with high density number and surface coverage. These slides were used as reference substrates to see in how far the scaling propensity could be compared between different material types (different assays). Crystal densities on the reference glass slides of the GOTS and PE assays were respectively 258 ± 22 and 87 ± 7 crystals/mm^2; the surface coverage were 19.5 ± 1.2% and 13.3 ± 0.8%. This shows that density and coverage can vary by as much as a factor ∼3 from one assay to the next for the same hydrophilic glass reference. Similar differences in nucleation/adsorption densities between different assays have been observed (on GOTS; compare Figure 5 and Figure S2). They most likely result from differences in the dynamics of $(NH_4)_2CO_3$ sublimation or dissolution, which could be due to temperature differences are unequal exposed area of $(NH_4)_2CO_3$ powder. These variations do not however challenge conclusions that can be inferred from the shape of $\sigma(t)$ and $s(t)$ within one assay (one batch of samples); also, systematic differences by a factor ≫3 in crystal densities between different assays should be interpreted as resulting from an intrinsic difference in the scaling propensity of the substrates, rather than mere fluctuations.

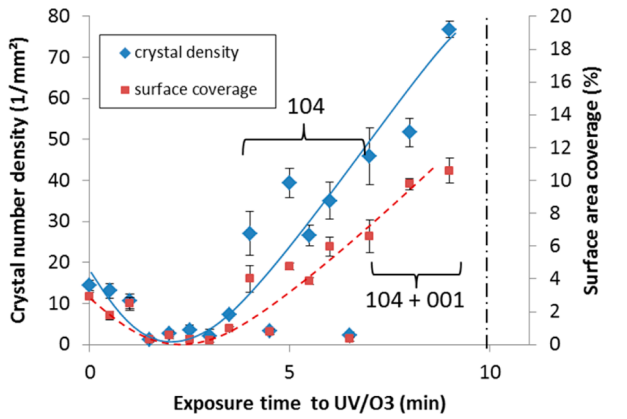

Figure 5. Mineralization results for GOTS. U-shaped lines are guides to the eye. The black vertical dash-dot line indicates the time at which the silane layer has been completely removed by the UV−O_3 exposure. "104" and "001" indicate exposure times for which these calcite orientations were predominant.

Silanized Glass (GOTS). Averaging over all samples, 90% of crystals found on GOTS were calcite, 10% vaterite. The vaterite fraction tended to decrease with increasing exposure time (data not shown). The ratio of ⟨104⟩ to ⟨001⟩ oriented crystals was measured[20] by X-ray diffraction in the $\theta-2\theta$ mode (Figure S4) and quantitatively confirms results obtained from optical microscopy inspection of the samples. At low exposure times, no preferred orientation of the calcite crystals was observed (Figure 4d). At intermediate exposure times (4−7 min), corresponding to contact angles 40°−70°, we observed complete ⟨104⟩ orientation of calcite crystals (Figure 4e). As the silane layer wore off at higher exposure times, ⟨001⟩ orientation started being prominent and was dominant (>85% of crystals) for wetting substrates ($\theta = 0°$, Figure 4f), just as for nonsilanized hydrophilic glass. The transition from no-orientation to ⟨104⟩ and eventually ⟨001⟩ with increasing exposure was further confirmed by placing a mask at a distance from GOTS, so that a half-light region was created. Exposing the substrates to UV/O_3 for 30 min gave rise to a continuous contact angle gradient across the mask boundary. ⟨104⟩ oriented crystals were predominantly seen at the mask boundary and ⟨001⟩ in the exposed region (Figure S1); no other orientations were observed.

Crystal number densities initially decreased as the substrate became more hydrophilic (Figure 5). As the silane wore off and ⟨104⟩ (intermediate t) and ⟨001⟩ (high t) orientations became more prominent, nucleation densities increased to eventually reach those of the reference glass substrates. $s(t)$ follows the same trend as $\sigma(t)$ as crystal size was fairly constant for the different samples. The same trends were reproduced in an independent mineralization assay (Figure S2).

Polyethylene (PE). For PE, we observed no preferred orientation of calcite crystals for all exposure times (Figure 4b,c). At low t, PE exhibited considerable amounts of vaterite (up to 50%, Figure 4b,c). Both the vaterite fraction (Figure 6b) and the total crystal number (Figure 6a) density decreased with increasing t. The disappearance of vaterite only partially accounted for the overall decrease of $\sigma(t)$. We also observe fluctuations of the crystal density and coverage for different sample exposure times. As these fluctuations could not be associated with any change in the polymorph or orientation of the crystals, the data are fitted by a least-squares linear fit to show the overall trend (it does not reflect any linear physical phenomenon). The same overall decreasing trend was checked in an independent mineralization assay (Figure S3) and found to be reproducible. Fluctuations could be due to inhomogeneities or adsorption of impurities to the sample surface; a way to reduce these fluctuations would be to increase the substrate surface area by using ground PE powder and measuring the $CaCO_3$ deposition rate (information on orientation would however be lost). The surface coverage $s(t)$ followed the same trend as $\sigma(t)$.

DISCUSSION

The major result of our research is that increasing the wettability by exposure to UV/O_3 lowers or even inhibits $CaCO_3$ deposition for all substrates that did not promote any particular crystalline orientation (PE and GOTS at low t). For all substrates, UV/O_3 also induced a rarefaction of vaterite that accounts only partially for the overall decrease of nucleation densities. We have further demonstrated that substrates that

dx.doi.org/10.1021/jp503807v | J. Phys. Chem. C XXXX, XXX, XXX−XXX

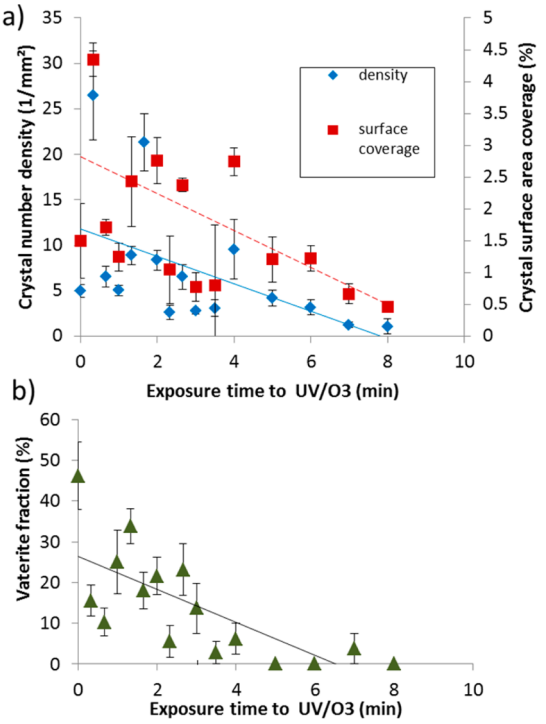

Figure 6. PE mineralization assay: (a) density and surface coverage; (b) vaterite fraction. Straight lines are least-squares linear fits of the data showing average trends.

strongly promote a given crystalline orientation (GOTS at intermediate time and glass) also result in higher crystal densities than surfaces that do not promote orientation: clean glass and highly oxidized OTS gave densities of ~150−250 and ~80−120 mm^{-2}, respectively, which is higher by a factor 4−12 than the densities on PE and native/mildly oxidized OTS which gave on average ~20 mm^{-2}. As crystal density differences on the reference glass slides for different batches (i.e., variability across different assays) only differed by up to a factor ~3, glass and highly oxidized OTS are clearly more potent inductors of $CaCO_3$ than PE and native/mildly oxidized OTS.

We now interpret our results within the frame of classical nucleation theory[21] (CNT), which was initially developed for ion-by-ion heterogeneous nucleation. Although we cannot ascertain whether the crystals we observe result from an ion-by-ion build-up or by bulk nucleation followed by adhesion, CNT provides a framework that can be applied to both mechanisms. It states that the nucleation rate J_0 (crystal surface density per unit time) depends on the supersaturation $\sigma = \ln(a_{Ca^{2+}}a_{CO_3^{2-}}/K_{sp})$ through

$$\ln(J_0) = \ln(A) - \frac{B}{\sigma^2} \quad (2)$$

where A is dependent on kinetic factors such as ion/nucleus fluxes to the substrate surface and barriers to ion desolvation; B is related to the net surface free energy given in eq 1 by

$$B = \frac{F\omega^2\gamma_{net}^{\ 3}}{(k_BT)^2} \quad (3)$$

where F is a nucleus shape factor, ω the molecular volume of crystals formed, k_B the Boltzmann constant, and T the temperature. The crystal density we measure in our experiment can be mathematically expressed by the integral of the nucleation rate over a ramp of supersaturation, the maximum of which lies in the range 6.2−7.6 (cf. Experimental Section). Both the kinetic barrier A and the interfacial free energies contained in B can potentially influence the crystal densities. Our experimental protocol, although efficient at isolating the influence of substrate surface chemistry on heterogeneous crystallization, does not allow us to dissociate contributions from these two terms. This would require monitoring the nucleation rate for each substrate at different supersaturation levels.[6,8] We will first interpret our data in terms of interfacial energy changes and give an a posteriori justification of why this seems reasonable.

The decreasing nucleation density vs hydrophilicity trend can be explained in the light of eq 3 and eq 1 for the net surface free energy of a $CaCO_3$ nucleus to a substrate γ_{net}. $\gamma_{CaCO_3/sol}$ is substrate-independent. $\gamma_{sub/sol}$ obviously decreases as the substrate is exposed to UV/O_3 and becomes more wettable. While the variation of $\gamma_{CaCO_3/sub}$ with exposure to UV/O_3 is a priori unknown, our observations of decreasing crystals densities (i.e., increasing γ_{net}) show that it should at least decrease less than $\gamma_{sub/sol}$. In other words, the formation of solution−substrate bonds could be favored over calcium carbonate−substrate bonds as the surfaces are exposed to UV/O_3. At low t, when −OH groups (Figure 3d) are dominant, the surface could for example be more prone to form hydrogen bonds with surrounding water molecules rather than carbonate ions.

At higher t, charged carboxylic groups appear on all substrate surfaces and are deprotonated at the pH values at which we perform our experiment (7−9.5). One can only speculate as to the effect of a statistically distributed surface charge on $CaCO_3$ nucleation: provided their density is sufficient, carboxylic groups could for example bridge divalent Ca^{2+} ions that could act as nucleation sites or attract positively charged $CaCO_3$ nuclei; inversely, they might also repel negatively charged $CaCO_3$ nuclei. As adsorption of bulk particles plays an important role in $CaCO_3$ scaling phenomena, an important step would be to measure the ξ-potential[22] of bulk-nucleated particles (the prenucleation clusters that have been evidenced by Gebauer et al.[23] and substrate surface to see whether any insight on the scaling propensity can be gained from simple electrostatic adhesion considerations).

We have further demonstrated that substrates that strongly promote a given crystalline orientation (GOTS at intermediate time and glass) also result in higher crystal densities than surfaces that do not promote orientation. This can be rationalized by considering that the selected crystals faces have lower $\gamma_{CaCO_3/sub}$ compared to other possible crystal faces and consequently a lower net surface free energy γ_{net}. This would explain the increase of crystal number densities for GOTS at intermediate and high t.

The interpretation of our results in terms of a decreased surface free energy of nucleation/adhesion corroborates and extends results of Bargir et al.[7] obtained on metals and recent findings by Giuffre et al.[8] on coatings of polysaccharides found in the organic matrix of oyster shells. Both of these investigators find that the net surface free energy of the $CaCO_3$ substrate−solution system decreases with increasing water contact angle (hydrophobicity). Using a very different experimental approach, we show here that this trend holds true for plastics and organic films and breaks down for surfaces that induce strong crystalline orientation.

dx.doi.org/10.1021/jp503807v | J. Phys. Chem. C XXXX, XXX, XXX−XXX

Although the a posteriori finding that our results follow trends similar to those found in the literature seems to justify an interpretation in terms of net surface free energy, we cannot exclude the possibility that the trends obtained could result from differences in the kinetic barrier A (eq 2) associated with the different samples. The most hydrophilic surfaces could for example chelate cations that could hinder the adsorption of precrystalline $CaCO_3$ clusters, or delay desolvation of the substrate for crystal attachment. In these examples, kinetic barriers would intuitively seem to scale with the net surface free energy. Giuffre et al.[8] have however shown the kinetic barrier and the surface free energy to be anticorrelated for polysaccharide surfaces in the supersaturation range σ = 5−5.8 (i.e., lower than the supersaturations considered in this work). The physical explanation of this anticorrelation and whether it holds true for other surface types such as those considered in this study remain to be elucidated.

We now briefly discuss possible causes of the striking orientations observed on GOTS at intermediate t (⟨104⟩) and on hydrophilic glass (⟨001⟩). XPS analysis shows that the substrates that promote ⟨104⟩ present roughly equal densities of alcohol, aldehyde, and carboxylic groups (Figure 3d, 6 min). As these are present on oxidized PE with similar densities but do not induce orientation, the mere presence of these moieties does not explain the observed behavior. The orientation of crystals on GOTS must therefore be either due to the well-determined orientation of each silane chain with respect to the surface in GOTS (stereochemical effect) or to the 2D organization of the silane surface (epitaxial effect). It has been shown for −OH-terminated thiols on gold[20] and C−NH_2 amine groups[24] that these effects could induce ⟨104⟩ orientation of calcite.

The ⟨001⟩ orientation of calcite on mica has been reported[25] and shown to be induced by the presence of nanometer-sized K_2CO_3 crystallites on freshly cleaved mica surfaces. The XPS peak at 289.5 eV which we attributed to COOH (288.9 eV) for GOTS could also, in the case of alkali containing glass coverslips, come from Na_2CO_3 (289.2 eV), $CaCO_3$ (289.5 eV) or K_2CO_3 (290.9 eV). All of these could potentially form as a result of reactions between Na_2O, K_2O, and CaO and atmospheric CO_2. The resulting carbonates could then act as nucleation seeds for further calcium carbonate growth. The negative surface charge beared by clean hydrophilic glass could also favor the nucleation of the Ca^{2+}-containing positively charged (001) plane: Duffy et al.[26] show that the ⟨001⟩ orientation is energetically favored for high energy polar substrates, such as the oxidized glass slides used in this study.

CONCLUSIONS

Wettability, chemical composition, and surface structure all influence the rate and mechanism of surface promoted crystal growth. We have demonstrated that varying wettability can influence the surface promoted nucleation/adsorption of $CaCO_3$ in two opposite ways, depending on whether or not crystalline orientation could be induced by our surface treatment:

(1) A nonspecific decrease of the crystal density with increasing surface wettability was observed substrates that did not promote a specific crystal orientation: polyethylene and mildly oxidized self-assembled OTS. This nonspecific effect can be rationalized by considering that, to be able to adsorb/nucleate to the substrate, a $CaCO_3$ particle must compete with pre-existing substrate−solution interactions (e.g., hydrogen bonds, electrostatic double layers).

(2) A substrate specific increase of the crystal density with increasing surface wettability was observed when UV/O_3 exposure also brought about highly selective crystal orientation. This was observed for highly oxidized self-assembled monolayers of OTS and glass. In these cases, UV/O_3 treatment induces structural changes that promote crystal orientation either by epitaxial or stereochemical effects.

The combination of these two aspects yields a more nuanced and detailed picture of the fascinating phenomenon of surface promoted crystal growth, corroborating and extending recent results obtained on polysaccharide coatings[8] and metals.[7] From an applied perspective, our research shows that simple hydrophilic treatments such as UV/O_3 or electron beam irradiation could be considered to lower the propensity of $CaCO_3$ to form scales. It is however clear that once scales have formed the effect of surface finish will be weakened. Further dedicated studies on industrial materials would therefore be required to assess whether such surface treatments can resist and put off nucleation or nucleus adhesion on time scales of several years.

ASSOCIATED CONTENT

Supporting Information

Mask experiments on GOTS samples confirming the observed orientation effect; independent additional mineralization assays performed on GOTS and PE; X-ray orientation analysis on GOTS. This material is available free of charge via the Internet at http://pubs.acs.org.

AUTHOR INFORMATION

Corresponding Author

*E-mail nico.chevalier@gmail.com.

Notes

The authors declare no competing financial interest.

ACKNOWLEDGMENTS

I thank P. Jégou (CEA/SPCSI) for help with the XPS measurements and analysis, C. Blot for helping with sample preparation, J.-F. Berret for proofreading the manuscript, C. Martel for her continued encouragements, P. Guenoun, C. Chevallard, and V. Fleury for giving me the opportunity to perform this work, and three anonymous reviewers for their insightful comments.

REFERENCES

(1) http://www.dutchnews.nl/news/archives/2009/04/philips_recalls_two_million_co.php.

(2) MacAdam, J.; Parsons, S. Calcium Carbonate Scale Formation and Control. *Rev. Environ. Sci. Bio/Technol.* **2004**, *3*, 159−169.

(3) Baker, J.; Judd, S. Magnetic Amelioration of Scale Formation. *Water Res.* **1996**, *30*, 247−260.

(4) Keysar, S.; Semiat, R.; Hasson, D.; Yahalom, Y. Effect of Surface Roughness on the Morphology of Calcite Crystallizing on Mild Steel. *J. Colloid Interface Sci.* **1994**, *162*, 311−319.

(5) Deng, H.; Shen, X.-C.; Wang, X.-M.; Du, C. Calcium Carbonate Crystallization Controlled by Functional Groups: a Mini-Review. *Front. Mater. Sci.* **2013**, *7*, 62−68.

(6) Hamm, L.; Giuffre, A.; Han, N.; Tao, J.; Wang, D.; De Yoreo, J.; Dove, P. Reconciling Disparate Views of Template-Directed Nucleation through Measurement of Calcite Nucleation Kinetics and Binding Energies. *Proc. Natl. Acad. Sci. U. S. A.* **2014**, *111*, 1304−1309.

(7) Bargir, S.; Dunn, S.; Jefferson, B.; Macadam, J.; Parsons, S. The Use of Contact Angle Measurements to Estimate the Adhesion Propensity of Calcium Carbonate to Solid Substrates in Water. *Appl. Surf. Sci.* **2009**, *255*, 4873−4879.
(8) Giuffre, A.; Hamma, L.; Han, N.; De Yoreo, J.; Dove, P. Polysaccharide Chemistry Regulates Kinetics of Calcite Nucleation Through Competition of Interfacial Energies. *Proc. Natl. Acad. Sci. U. S. A.* **2013**, *110*, 9261−9266.
(9) Dey, A.; Bomans, P.; Müller, F.; Will, J.; Frederik, P.; de With, G.; Sommerdijk, N. The Role of Prenucleation Clusters in Surface-Induced Calcium Phosphate Crystallization. *Nature* **2010**, *9*, 1010−1014.
(10) Rieke, P. Selection of Phase and Control of Orientation during Physisorption on Surfaces of Homogeneously Formed Calcium-Carbonate Nuclei. *Mater. Sci. Eng., C* **1995**, *2*, 181−189.
(11) Recent investigations have shown that the mineral phase often nucleates first as an isotropic ionic-liquid-like amorphous compound.[27] In this case a single value of tension for each pair of interfaces is sufficient to describe the adhesion/nucleation behavior.
(12) Aizenberg, J.; Black, A.; Whitesides, G. Control of Crystal Nucleation by Patterned Self-Assembled Monolayers. *Nature* **1999**, *398*, 495−498.
(13) Fricke, M.; Volkmer, D. Crystallization of Calcium Carbonate Beneath Insoluble Monolayers: Suitable Models of Mineral-Matrix Interactions in Biomineralization. *Top. Curr. Chem.* **2007**, *270*, 1−41.
(14) http://bigwww.epfl.ch/demo/dropanalysis/.
(15) Liu, P.-H.; Thebault, P.; Guenoun, P.; Daillant, J. Oxidation of Alkylsilane-Based Monolayers on Gold. *Macromolecules* **2009**, *42*, 9609−9612.
(16) Note that for exposure times comprised between 1 and 6 min, the total functional group densities computed exceeds the initial CH_3 surface density. This indicates that the functional groups are present not only at the surface of the silane, but also presumably in the layers directly below the surface.
(17) Poulsson, A.; Mitchell, S.; Davidson, M.; Johnstone, A.; Emmison, N.; Bradley, R. Attachment of Human Primary Osteoblast Cells to Modified Polyethylene Surfaces. *Langmuir* **2009**, *25*, 3718−3727.
(18) Mitchell, S.; Poulsson, A.; Davidson, M.; Emmison, N.; Shard, A.; Bradley, R. Cellular Attachment and Spatial Control of Cells using Micro-Patterned Ultra-Violet/Ozone Treatment in Serum Enriched Media. *Biomaterials* **2004**, *25*, 4079−4086.
(19) Hu, Q.; Nielsen, M.; Freeman, C.; Hamm, L.; J, T.; Lee, J.; Han, T.; Becker, U.; Harding, J.; Dove, P.; De Yoreo, J. The Thermodynamics of Calcite Nucleation at Organic Interfaces: Classical vs. Non-Classical Pathways. *Faraday Discuss.* **2012**, *159*, 509−523.
(20) Aizenberg, J.; Black, A.; Whitesides, G. Oriented Growth of Calcite Controlled by Self-Assembled Monolayers of Functionalized Alkanethiols Supported on Gold and Silver. *J. Am. Chem. Soc.* **1999**, *121*, 4500−4509.
(21) Nielsen, A. *Kinetics of Precipitation*; Macmillan: New York, 1964.
(22) Moulin, P.; Roques, H. Zeta Potential Measurement of Calcium Carbonate. *J. Colloid Interface Sci.* **2003**, *261*, 115−126.
(23) Gebauer, D.; Völkel, A.; Cölfen, H. Stable Prenucleation Calcium Carbonate Clusters. *Science* **2008**, *322*, 1819−1822.
(24) Archibald, D.; Qadri, S.; Gaber, B. Modified Calcite Deposition Due to Ultrathin Organic Films on Silicon Substrates. *Langmuir* **1996**, *12*, 538−546.
(25) Stephens, C.; Mouhamad, Y.; Meldrum, F.; Christenson, H. Epitaxy of Calcite on Mica. *Cryst. Growth Des.* **2010**, *10*, 734−738.
(26) Duffy, D.; Harding, J. Simulation of Organic Monolayers as Templates for the Nucleation of Calcite Crystals. *Langmuir* **2004**, *20*, 7630−7636.
(27) Demichelis, R.; Raiteri, P.; Gale, J.; Quigley, D.; Gebauer, D. Stable Prenucleation Mineral Clusters Are Liquid-Like Ionic Polymers. *Nat. Commun.* **2011**, *2*, 590.